Available online at www.sciencedirect.com
ScienceDirect
Journal of Sound and Vibration 305 (2007) 596–613
JOURNAL OF SOUND AND VIBRATION
www.elsevier.com/locate/jsvi

Non-contact vibration control system employing an active eddy current damper

Henry A. Sodano[a,*], Daniel J. Inman[b]

[a]Department of Mechanical Engineering, Engineering Mechanics, Michigan Technological Institute, 815 R.L. Smith ME-EM Building, 1400 Townsend Drive, Houghton, MI 49931-1295, USA
[b]Center for Intelligent Material Systems and Structures, Virginia Polytechnic Institute and State University, Blacksburg, VA 24061-0261, USA

Received 9 September 2005; received in revised form 30 March 2007; accepted 13 April 2007
Available online 27 June 2007

Abstract

When a conductive material is subjected to a time-changing magnetic field, eddy currents are formed in the conductor. These currents circulate inside the conductor such that a magnetic field is formed. This eddy current field then interacts with the applied field resulting in a dynamic force between the conductor and the magnetic source. The force can be considered dynamic because as the eddy currents circulate inside the conductor they are dissipated by the internal resistance of the conductor. Therefore, if a continuously changing field is not applied to the conductor the force will disappear. However, the eddy current forces can be utilized to form an actuator by applying a time-changing current to an electromagnet that is in close proximity to a conductive material. This actuation method is easy to incorporate into the system and allows significant forces to be applied without every coming into contact with the structure. In this manuscript, the authors develop the concept and show that it can be accurately modeled and effectively used to control the vibration of a structure. The active eddy current actuator has not been previously demonstrated and therefore this article will present the first use of the system for providing transverse vibration suppression. Furthermore, the constraints necessary to design an active control filter will be presented. This vibration control system will use a velocity feedback filter to actively modify the current applied to the coil. Using this system, experiments are performed on a cantilever beam showing the system can effectively suppress each of the first five modes of vibration by upwards of 20 dB, demonstrating the actuator has an increased bandwidth over previously used eddy current methods.

1. Introduction

Eddy currents can be induced in a conductive material by actively changing the strength of the field surrounding the conductor. These eddy currents then circulate inside the conductor resulting in a magnetic field that interacts with the applied field to generate a magnetic force. By actively controlling the current flowing through an electromagnetic coil, this force can be utilized for a number of different applications. In the present study, an electromagnet is used to actively suppress the vibration of a structure. However, the concept

*Corresponding author. Tel.: +1 906 487 2709; fax: +1 906 487 2822.
E-mail addresses: hsodano@mtu.edu (H.A. Sodano), dinman@vt.edu (D.J. Inman).

0022-460X/$ - see front matter © 2007 Elsevier Ltd. All rights reserved.
doi:10.1016/j.jsv.2007.04.050

of using the eddy currents generated in a conductive material that experiences a time-changing magnetic field for the purpose of increasing system damping has been studies by several researchers. For instance, Karnopp [1] introduced the idea that a linear electrodynamic motor consisting of coils of copper wire and permanent magnets could be used as an electromechanical damper for vehicle suspension systems. It was shown that this actuator could be much smaller and lighter than conventional dampers while still providing effective damping in the frequency range typically encountered by road vehicle suspension systems; however, it was unable to effectively isolate the vehicle from shock excitation. Schmid and Varga [2] studied a vibration-reducing system with eddy current dampers (ECDs) for high resolution and nanotechnology devices such as a scanning tunneling microscope (STM). Teshima et al. [3] investigated the effects of an ECD on the vibrational characteristics of superconducting levitation and showed that the damping of vertical vibrations was about 100 times improved by ECDs.

More recently, Kwak et al. [4] investigated the effects of an ECD on the vibration of a cantilever beam and their experimental results showed that the ECD can be an effective device for vibration suppression. The eddy currents were induced in this system due to the relative motion between a permanent magnet attached to a flexible linkage and a copper conducting plate, both located at the tip of the beam. Later, Bae et al. [5] modified and developed the theoretical model of the ECD constructed by Kwak et al. [4]. Using this new model, the authors investigated the damping characteristics of the ECD and numerically simulated the vibration suppression capabilities of a cantilever beam with an attached ECD.

Typical ECDs configure the motion of the conductor perpendicular to the poling axis of the magnet [6]. Sodano et al. [7] developed a new magnetic damping system that differed from others because the motion of the conductor was along the poling axis of the magnet rather than perpendicular to it. A new damping method was developed in this study that placed a single permanent magnet in close proximity with a conductive patch mounted to the surface of a vibrating structure. The eddy currents were induced in the conductor due to the vibration of the beam in the magnetic field. The system was modeled and experiments were performed to shown the model could accurately predict the damping induced within ten percent. Additionally, it was shown that the damper could generate damping ratios as high as 35% of critical on the cantilever beam tested. This damper had one very advantageous trait; it was completely non-contacting. Therefore, the damper could be applied to a variety of structures without inducing mass loading or added stiffness, which are downfalls of other damping techniques. This allows the damper to be applied to extremely flexible structures without inducing surface irregularities. However, the density of the currents induced in the conductor is directly proportional to its thickness, raising the question of whether sufficient forces could be induced in a thin membrane to suppress its vibration. Therefore, Sodano et al. [8] investigated the use of the ECD of Ref. [7] for the suppression of vibrations occurring in the ultra large membrane mirrors and antennas desired for use in future satellite applications. The authors modeled the system and experiments were performed in both ambient and vacuum conditions to identify the accuracy of the model and show the functionality of the ECD at vacuum pressure. It was found that the ECD could indeed suppress the vibration of the membrane and that the model could effectively predict the damping ratio of the first mode. With the ECD present the membrane had damping as high as 30% of critical at ambient pressure and 25% of critical at vacuum pressure. Additionally, the variation in damping between ambient and vacuum pressure was shown to occur due to air damping.

Building on the damping system described in Sodano et al. [7], used the idea that the radial magnetic flux was responsible for the generation of eddy currents to improve the previous damper's effectiveness; this work is reported in Ref. [9]. To increase the magnitude of the radial magnetic flux applied to the beam, a second magnet was placed on the other side of the beam such that the two magnetic poles facing each other were of opposite polarity. As the two magnets approach each other, the radial magnetic field is intensified causing an increase in the damping force. From experiments performed on a cantilever beam it was found that with the additional radial magnetic flux, 130% of critical damping could be achieved. In addition to improving the effectiveness of the eddy current damping mechanism, Sodano et al. [9] improved the accuracy of the mathematical model through the use of the image method to meet the electrical boundary conditions of the conductor. By enforcing the electrical boundary conditions the accuracy of the predicted damping increased by more than 5%.

In the aforementioned studies, the eddy currents are generated because of to the motion of the conductor relative to the magnetic source. A novel concept was developed by Sodano et al. [10], in which the magnet was

moved relative to the vibrating structure, such that both the motion of the conductor and the motion of the magnet were along the poling axis. This system could function as a passive damper if the magnet were left stationary or as an active damper if the magnet is moved relative to the structure. A feedback control system was developed such that the motion of the permanent magnet was dependent on the velocity of the structure. Using this system, it was shown that significant control forces could be applied to the structure allowing the first mode of vibration to be suppressed by upwards of 95%. This study represented the first application of an active eddy current damping system applied to a harmonic system (previous applications were applied to rotating systems).

An electromagnet can be used to generate eddy currents in a structure if the current flowing through it is actively varied such that a time varying magnetic field is formed. The use of an electromagnet with a time-changing current to induce eddy currents has been previously studied, but only in order to see the structural response of a system subjected to the changing field. For instance, Tani et al. [11], Morisue [12], Tsuboi et al. [13], Takagi et al. [14] and Takagi and Tani [15] have all analyzed the response of a conducting plate subjected to impulsive magnetic fields. Each of these researchers has applied upwards of 1000 amps to an electromagnet and predicted the dynamic response. Additionally, Lee [16] investigated the stability of electrically conducting beam-plates when subjected to transverse magnetic fields and showed that three stability regions existed. Because the use of an electromagnet for the purpose of generating eddy current forces to control vibrations had not been studied, Sodano et al. [17] modeled and simulated the case, where an electromagnetic is used to generate an eddy current force in a structure for vibration suppression. The predicted and experimentally verified that when using a time-changing current to induce eddy currents in the conductor, the force induced is at twice the frequency of the current applied. Using this effect, a controller was designed to reduce the sensing signal's frequency by half such that the control force was at the same frequency as the structure. Using this algorithm the feedback control system was numerically simulated showing the control system to be effective in suppressing the structural vibration.

In the study presented here, experimental testing of the active eddy current damping system proposed by Sodano and Inman [17] is described. The configuration of the electro-mechanical system is shown in Fig. 1. An electromagnet is located a small distance from a cantilever beam with a conductive patch bonded to it. The motion of the cantilever beam is along the poling axis of the magnet and therefore subjects the conductor to a transverse magnetic field, causing the resulting eddy current force to be developed both due to the motion of the conductor and the time varying current applied to the electromagnet. A non-contacting sensor was used to measure the velocity of the vibrating structure and a feedback controller was designed to suppress the vibration of the beam. In the experiments, it was found that the eddy current damping system can effectively suppress the transverse vibration of a beam and the model will be demonstrated to be accurate. This actuation system has only been previously proposed and not implemented. Therefore, this study provided the first demonstration that an active eddy current system can be used as a means to suppress the transverse vibrations.

2. Model of active eddy current system

2.1. Model of eddy current force

For an active damper that utilizes an electromagnet, the eddy currents formed due to the varying current applied to the coil and the motion of the beam must be included in the prediction of the eddy current density. As derived in Ref. [17], the eddy current density of the system is defined as

$$\mathbf{J} = \sigma\mathbf{E} = \sigma\left[(\mathbf{v}\times\mathbf{B}) - \frac{\partial\mathbf{A}}{\partial t}\right] = \sigma\left[v_z(-B_y\mathbf{i} + B_x\mathbf{j}) - \frac{\partial\mathbf{A}}{\partial t}\right], \tag{1}$$

where σ is the conductivity of the circuit, $\mathbf{A}$ the magnetic potential, B the magnetic flux density in the x- and y-direction, and v_z the velocity of the beam in the z-direction. To calculate the eddy current density, the magnetic flux density and the magnetic potential are required. The magnetic flux density of a cylindrical permanent magnet was derived by Sodano et al. [12] and can be modified to represent the flux in the radial or

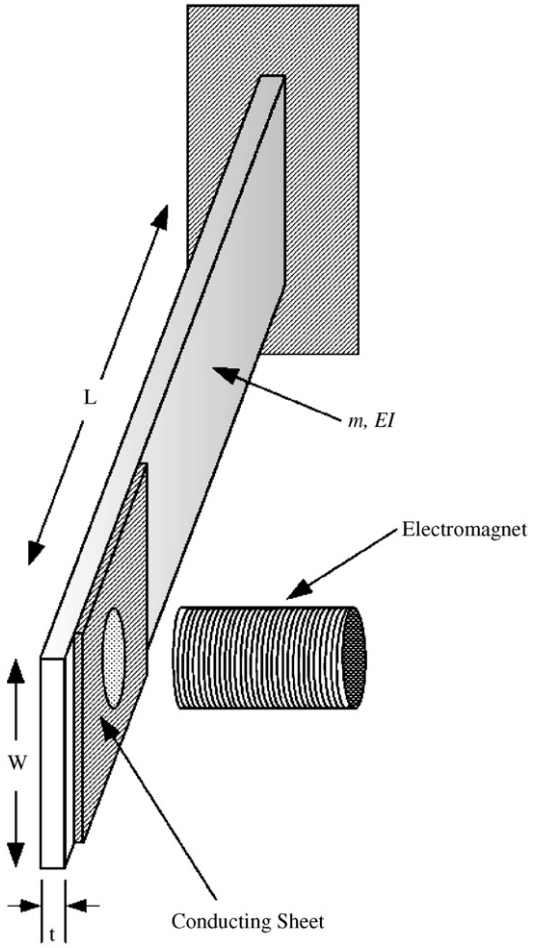

Fig. 1. Schematic showing the configuration of the active eddy current damper.

y-direction and the z-direction of an electromagnetic coil by the following equations:

$$B_y(y,z,t) = \frac{\mu_0 I(t) b}{4\pi} \int_{-L}^{0} (z - z') I_1(b, y, z - z')\, \mathrm{d}z', \tag{2}$$

$$B_z(y,z,t) = \frac{\mu_0 I(t) b}{4\pi} \int_{-L}^{0} I_2(b, y, z - z')\, \mathrm{d}z', \tag{3}$$

where z' and L are the distance in the z-direction and the length of the circular magnet, respectively, and the terms I_1 and I_2 are defined in Appendix A. As shown in Fig. 2, the magnetic flux distributions in Eqs. (2) and (3) are symmetric about the z-axis due to the symmetry of the circular magnet. The magnetic potential must be defined before the eddy current density can be determined and is written for a cylindrical magnet as

$$A_\phi = \frac{\mu_0 I(t) b}{4\pi} \int_{-L}^{0} \int_{-\pi/2}^{\pi/2} \frac{\sin\,\phi}{\sqrt{b^2 + y^2 + (z' - z)^2 - 2yb\,\sin\,\phi}} \mathrm{d}\phi\, \mathrm{d}z'\, \hat{\mathbf{a}}_\phi. \tag{4}$$

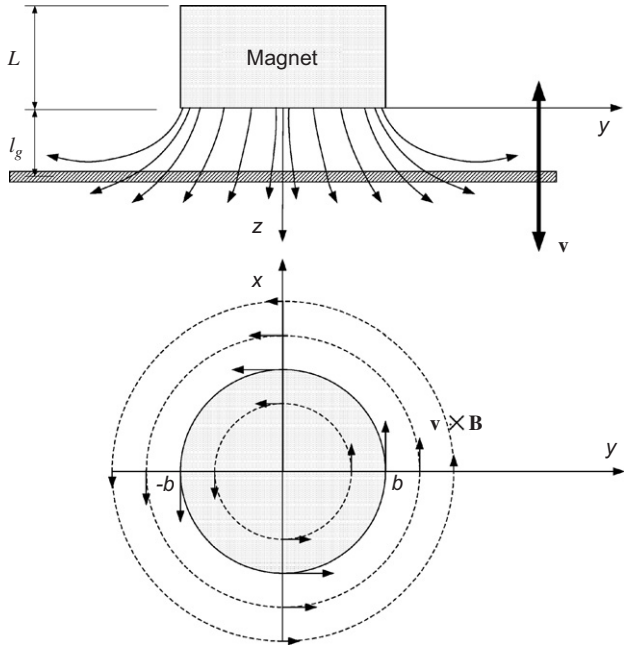

Fig. 2. Magnetic field and the eddy currents induced in the cantilevered beam.

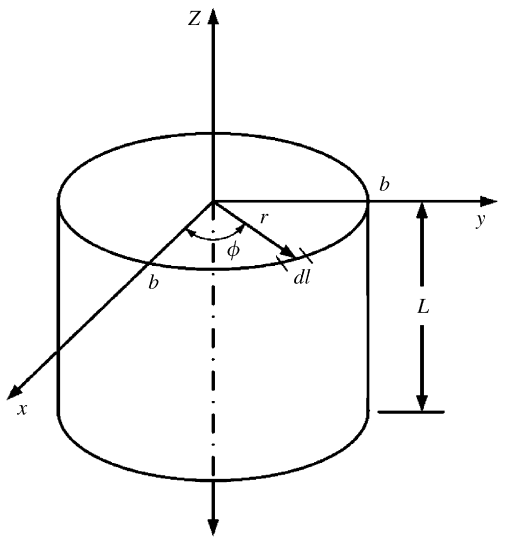

Fig. 3. Coordinate system used for the analysis.

It should be expected that the magnetic potential only be in the angular direction because the magnetic flux density, which is only in the radial and poling direction, is defined as the curl of the potential (the cross-product of a vector only in the angular direction will result in a new vector only in the radial and vertical directions). The coordinate system used to define Eqs. (2)–(4) is shown in Fig. 3, along with the position of the magnet relative to the origin.

Eq. (4) can now be used along with Eqs. (2) and (3) to calculate the eddy current density of Eq. (1). After solving for the eddy current density the force resulting form the eddy currents can be determined by

$$\begin{aligned}\mathbf{F} &= \int_V \mathbf{J}\times\mathbf{B}\,\mathrm{d}V \\ &= \sigma\delta\left[\int_0^{2\pi}\int_0^{r_c} y\frac{\partial A_\phi}{\partial t}B_y(y,l_g)\,\mathrm{d}y\,\mathrm{d}\phi - v\int_0^{2\pi}\int_0^{r_c} yB_y^2(y,l_g)\,\mathrm{d}y\,\mathrm{d}\phi\right]\hat{\mathbf{a}}_z \\ &= 2\pi\sigma\delta\left[\int_0^{r_c} y\frac{\partial A_\phi}{\partial t}B_y(y,l_g)\,\mathrm{d}y - v\int_0^{r_c} yB_y^2(y,l_g)\,\mathrm{d}y\right]\hat{\mathbf{a}}_z,\end{aligned} \tag{5}$$

where δ and v are the thickness and the vertical velocity of the conducting sheet, respectively, r_c the equivalent radius of the conductor that preserves its surface area, and l_g the distance between the conducting sheet and the bottom of magnet as was shown in Fig. 2. When the damping force is included into the equation of motion of the beam, it is split into two terms, one defining the force due to a transformer emf and the second due to a motional EMF. Eq. (5) contains two integrals, the first defines the transformer EMF, or the force due to the time-changing magnetic field and the second integral defines the motional EMF, or the eddy current damping force due to the beam's velocity in the magnetic field. The transformer force must be included as an external force and the motional force can be included as a viscous damping term due to its dependence on the velocity of the beam.

The force generated by actively controlling the strength of the magnetic field, results in an interesting effect: the frequency of the force applied to the beam is twice the frequency of the current applied to the coil. This effect is due to the trigonometric identity that states the product of a sine and cosine wave results in a sine wave at twice the frequency of the two waves. This identity appears in the first integral in Eq. (5) defining the transformer portion of the eddy current damping force as the product of the derivative of the magnetic potential and the magnetic flux density. It may not be immediately apparent that this effect occurs until it is realized that the magnetic flux density and magnetic potential are both a function of the time-dependent current applied to the electromagnet. This force frequency doubling effect has serious consequences that affect the design and performance of the active eddy current control system, and will be discussed in Section 4 of this paper.

2.2. Inclusion of active damping in beam equation

The dynamics of the structure can be coupled to the eddy current forces to predict the response of the structure. By using the assumed modes method, the equations of motion for a beam can be written in matrix form as follows:

$$\mathbf{M}\ddot{r}(t) + \mathbf{C}\dot{r}(t) + \mathbf{K}r(t) = \int_0^L f(x,t)\,\underline{\phi}(x)\,\mathrm{d}x + \sum_{i=1}^{p} F_i(t)\,\underline{\phi}(x_i), \tag{6}$$

where the mass matrix $\mathbf{M}$, the damping matrix $\mathbf{C}$, and the stiffness matrix $\mathbf{K}$ are defined by

$$\mathbf{M} = m_{ij} = \int_0^L \rho(x)\,\underline{\phi}(x)^{\mathrm{T}}\,\underline{\phi}(x)\,\mathrm{d}x, \tag{7}$$

$$\mathbf{K} = k_{ij} = \int_0^L EI(x)\,\underline{\phi''}(x)^{\mathrm{T}}\,\underline{\phi''}(x)\,\mathrm{d}x, \tag{8}$$

$$\mathbf{C} = c_{ij} = \int_0^L \phi(x)^{\mathrm{T}} c_b \phi(x)\,\mathrm{d}x, \tag{9}$$

where E is the modulus of elasticity, I the beam's moment of inertia, ρ the area density of the beam, c_b the beam's damping coefficient, $f(x,t)$ the distributed forces, F_i the concentrated forces, and $\phi(x)$ the assumed mode shape of the beam. As mentioned in the previous section, one term is modeled as a concentrated external force, while the other is modeled as a viscous damping force. The eddy current force due to the transformer

emf is included as a concentrated force and can be written as

$$F_1(t)\,\underline{\phi}(x_1) = F_T = \left[2\pi\sigma\delta \int_0^{r_c} y \frac{\partial A_\phi}{\partial t} B_y \,\mathrm{d}y\right] \underline{\phi}(x_e), \tag{10}$$

where F_T is the transformer eddy current force and $\phi(x_e)$ is the magnitude of the mode shape at the location of the ECD. The eddy current damping coefficient due to the motional EMF, can be arrived at by dividing the motional damping force of Eq. (5) by the beam's velocity, or written as follows:

$$F_2(t)\,\underline{\phi}(x_2) = c_e\,\underline{\phi}(x_e)\dot{r}(t), \tag{11}$$

where c_e is the eddy current damping coefficient defined as

$$c_e = \frac{F_M}{v_z} = -2\pi\,\sigma\,\delta \int_0^{r_c} y B_y^2(y, l_g)\,\mathrm{d}y, \tag{12}$$

where F_M is the motional eddy current force. Eqs. (10) and (11) show that the active ECD generates both a viscous damping force and a control force. As with the passive [6] and passive–active vibration control methods [10], the damping force is nonlinear with respect to the distance between the magnet and beam. In previous studies, the analysis of the damping effect through eddy currents was linearized, while in the case of the active system considered here, the system will not be linearized and will be simulated numerically. Substitution of Eqs. (7)–(11) into Eq. (6) defines the interaction between the beam and the active ECD.

3. Experimental setup of active damping system

To validate the accuracy of the active eddy current actuator model, an experimental analysis was performed on a cantilever aluminum beam. The dimensions of the beam used in these experiments are identical to those used by Sodano et al. [17] to verify the functionality of the method and are shown in Fig. 4. The electromagnet used in the experiments was fabricated by hand in the Center for Intelligent Material Systems and Structures (CIMSS) using 26 gauge copper wire and a soft iron core. The coil had a 25.4 mm diameter and was 50.8 mm long. The material properties of the beam, conductor and electromagnet are provided in Table 1.

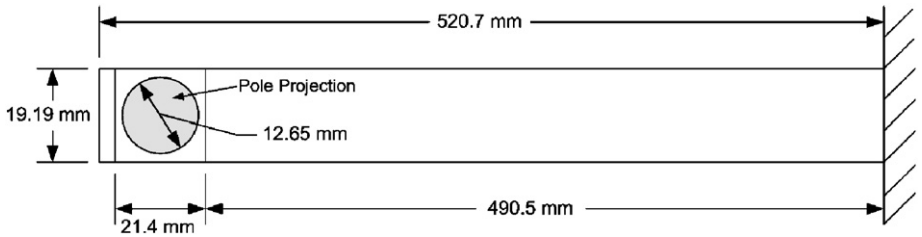

Fig. 4. Schematic showing the dimensions of the beam.

Table 1
Physical properties of the beam, conductor and magnet

Property	Value
Young's modulus of beam	75 Gpa
Density of beam	2700 kg/m^3
Conductivity of aluminum beam	$3.82 \times 10^7\,\Omega$/m
Thickness of copper conductor	0.62 mm
Conductivity of copper conductor	$5.80 \times 10^7\,\Omega$/m
Relative permeability of core material	1500
Number of turns in coil	1534 turns
Resistance of coil	13.8 Ω

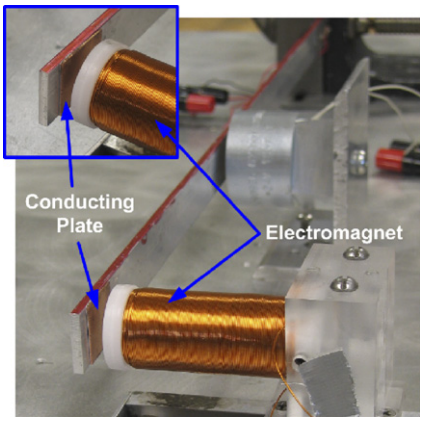

Fig. 5. Experimental setup of active eddy current damper.

In order to induce eddy currents in the conductive beam, the current applied to the electromagnetic coil is actively controlled. In doing so, the magnetic field applied to the beam is changed such that the density of the eddy currents and the force applied to the beam can be modified to suppress the motion of the beam without contacting it. The experimental setup used to validate the model and demonstrate the performance of the active ECD is shown in Fig. 5, and consisted of a cantilever aluminum beam, an electromagnet used to apply a time varying magnetic field to the conductive beam and a Polytec laser vibrometer used as the velocity feedback sensor. The control scheme was implemented using a dSpace real-time control board, which allowed the controller dynamics to be implemented from Matlab's Simulink program. Using this controller, the gain could be modified in real time allowing the ideal value to be determined.

Two types of disturbances were applied to the beam and the controller was used to reject them. The first was a continuous harmonic excitation over a range of frequencies that was generated through a piezoelectric patch mounted at the root of the beam. The second disturbance was an initial displacement, which was applied using an electromagnet. By energizing the electromagnet, the beam is attracted to it resulting in an initial displacement, and when de-energized, the beam is released to vibrate freely. Because aluminum is not ferromagnetic, a 0.05 mm steel plate was attached to the side of the beam allowing the beam and electromagnet to interact. This system allowed a constant initial displacement to be repeatedly applied over numerous tests.

4. Discussion of results from model and experiments

4.1. Controller design

A positive feedback control system [18] was designed such that the current flowing through the electromagnet could be actively modified and the vibration suppressed. A block diagram representation of the closed-loop dynamics of the system with the active control system is presented in Fig. 6. This figure illustrates the manner in which the sensor signal is applied to the control system and the resulting force due to the current output of the controller. Additionally, in Fig. 6 the source of the nonlinearities that are present in the system due to the conversion of the control current into eddy currents in the conducting structure is shown. Due to the frequency doubling effect of the force applied to the beam, described in detail in Section 2.1, the controller must apply a force at half the sensed frequency. So that the force applied to the beam is at the same frequency as its vibration. This can be accomplished by dividing the frequency of the sensed vibration signal by half, which in principle can be accomplished as in the following expression:

$$\left|\sin\left(\frac{1}{2}\omega t\right)\right| = \sqrt{\frac{\omega}{2}\int_0^t \sin(\omega t)\,\mathrm{d}t}, \tag{13}$$

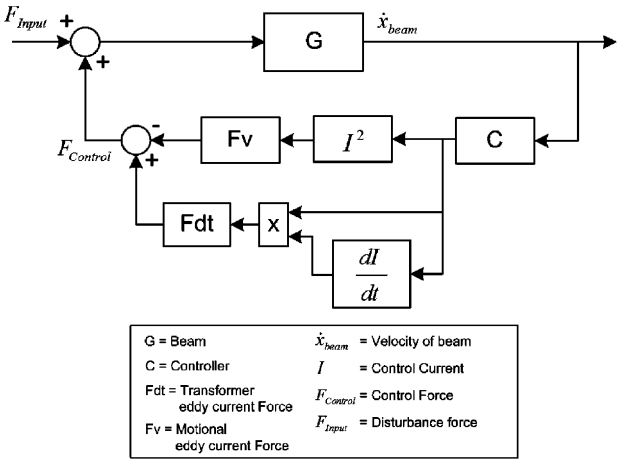

Fig. 6. Block diagram of feedback control system.

where ω is the frequency of the harmonic signal. This equation is applied to the output of the control filters which were designed for each mode. The feedback controller is a second order filter with three parameters chosen to provide the greatest vibration suppression to the frequency response. Two separate filter designs were used and are defined as

$$\frac{K\omega_f^2 s}{s^2 + 2\zeta_f \omega_f s + \omega_f^2}, \tag{14}$$

$$\frac{K\omega_f^2 s^2}{s^2 + 2\zeta_f \omega_f s + \omega_f^2}, \tag{15}$$

where K is the controller gain, ω_f the filter frequency and ζ_f the filter damping ratio. The filter defined in Eq. (14) is used to apply control to the first mode but the second mode, is controlled using the filter defined in Eq. (15). Both compensators defined in Eqs. (14) and (15) contain an extra zero in the numerator to account for the integration used in Eq. (13) to reduce the frequency of the sensing signal by half. The filter of Eq. (15) contains an additional zero to account for the phase shift of the electromagnet.

4.2. Tuning of the controller

Once the controllers were designed, the appropriate filter properties had to be identified. As mentioned, the second-order filter had three parameters, the filter damping ratio, filter frequency and control gain, which needed to be determined in order to maximize the damping added to the structure. These three parameters were determined by studying the frequency response as each parameter was individually varied. The process of identifying the filter frequency and filter damping for the first mode is illustrated in Figs. 7 and 8, respectively. From results in Fig. 7, it can be seen that as the filter frequency is adjusted, the frequencies affected by the controller are modified and Fig. 8 shows that the damping ratio can be adjusted until the peak is reduced to a minimum value. It is apparent from these two figures that the controller's performance can be visually inspected, and through an intuitive adjustment can be tailored to provide the desired response.

4.3. Results of model and experiments

Once the filters have been tuned to apply the maximum control to each targeted frequency, the performance of the new active eddy current control system and the accuracy of the modeling techniques can be demonstrated through a comparison of experimental and analytical results. Each controller is a second-order filter that applies vibration suppression to a narrow band of frequencies, typically located around one of the

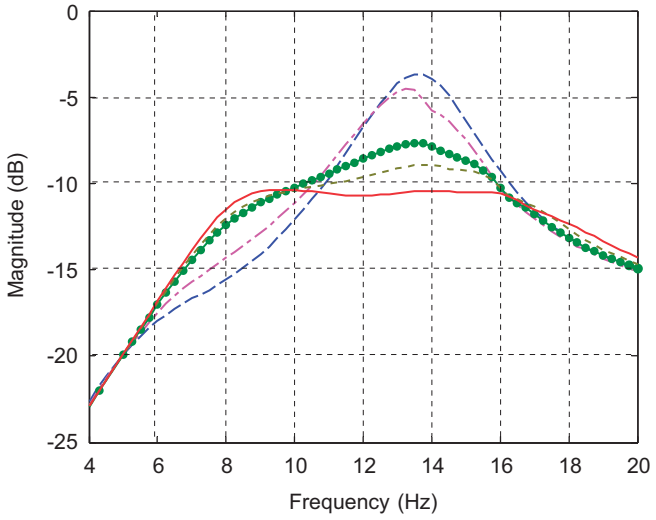

Fig. 7. Effect of varying the filter frequency on the frequency response. --, $0.77\omega_n$, -•-, $0.85\omega_n$, -●-, $1.1\omega_n$, ••, $1.2\omega_n$, and -, $1.35\omega_n$.

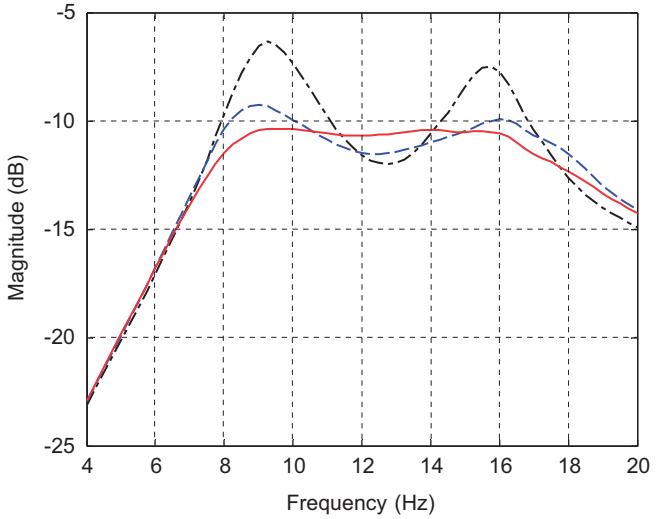

Fig. 8. Effect of varying the filter damping ratio on the frequency response. -•-, $\zeta_f = 0.2$; --, $\zeta_f = 0.4$; -, $\zeta_f = 0.6$.

system's natural frequencies; therefore, if multiple modes of vibration are to be controlled, each filter must be designed separately. The magnitude of a second-order filter rolls off at frequencies higher than the filter's natural frequency, thus allowing each filter to have little effect on higher modes but can lead to spillover and destabilization at lower frequencies. To avoid these negative effects, it is standard that the higher mode controllers are designed first. To demonstrate the accuracy of the theoretical model, both the frequency response and the time response of the system will be experimentally measured and predicted through a numerical simulation.

Because the effect of tuning of the controller can be most easily seen in the frequency response, we will begin by comparing the predicted and measured frequency response of the closed-loop system. Typically before multiple modes are controlled it is advantageous to apply control to each mode separately, thus identifying trends in the filter parameters and modes that may have little controllability, before compiling the entire group of filters together and attempting to tune them. Therefore, in the following plots showing the predicted and measured frequency response, the predicted response was tuned first to obtain the rough location of the

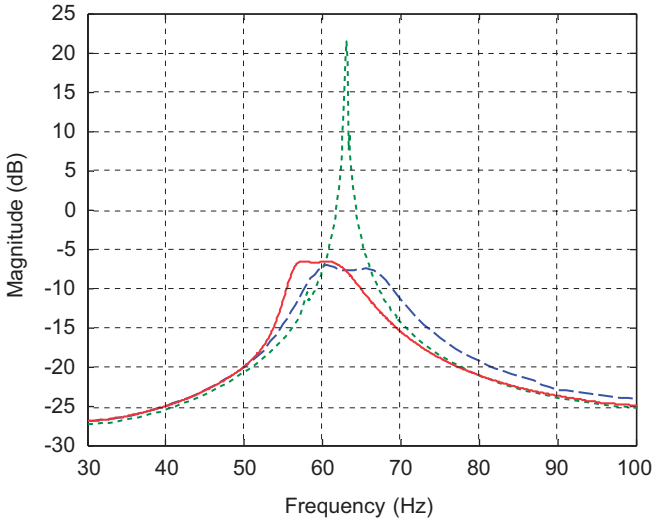

Fig. 9. Frequency response of second mode for controlled system compared to the case that no damping is added. ••, measured uncontrolled response, --, measured controlled response, and -, predicted controlled response.

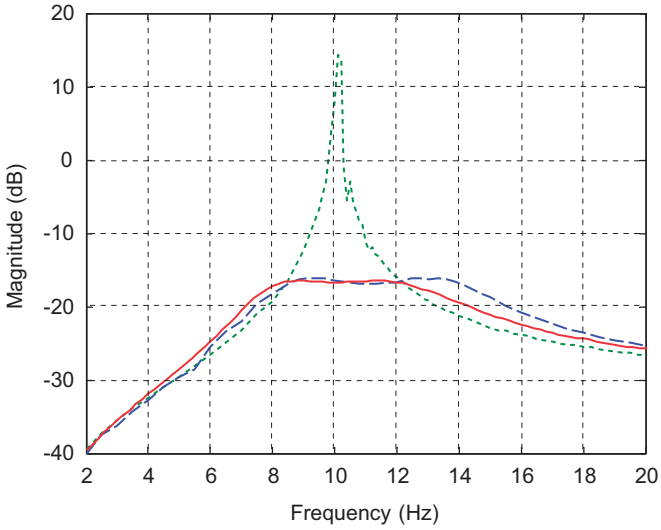

Fig. 10. Frequency response of first mode for controlled system compared to the case that no damping is added. ••, measured uncontrolled response, --, measured controlled response, and -, predicted controlled response.

experimental parameter allowing the experimental filters to be quickly adjusted. During testing, the sensor signal was first integrated then the square root was taken, resulting in a signal at half the measured frequency.

First, the frequency response of the active control system when applied to a single mode will be predicted and compared to the experimental data. For comparison, in Figs. 9 and 10 the measured and predicted closed-loop frequency response of the second and first mode are plotted along with the uncontrolled response of the beam. From these two figures it is evident that the active eddy current control system can effectively apply vibration suppression to the cantilever beam. The control system provides the second mode, shown in Fig. 9, with approximately 29 dB (approximately 96.6% suppression) reduction in vibration and the first mode, shown in Fig. 10, with approximately 30.5 dB (greater than 97% suppression) reduction in vibration. These results indicate the effectiveness of this new non-contact actuation system; however it can be seen in Fig. 9 that the predicted response of the second mode contains a 4 Hz reduction in the natural frequency with the controller which is not present in the measured response.

The shift in the peak of the predicted controlled natural frequency, which can be seen in Fig. 9, indicates that some of the system's dynamics are not modeled. Because each piece of equipment in the experimental setup had been included in the numerical simulation, it was determined that the model inaccuracy resulted form the electromagnetic coil. To identify if the magnetic field generated by the coil when subjected to a dynamic current was responsible for the model error, an experiment was performed to determine the characteristics of the transfer function between the current applied to the electromagnet and the magnetic field generated. The experiment did not consist of an ideal setup due to the unavailability of a gaussmeter to measure the actual magnetic field developed by the coil. However, a permanent magnetic was mounted to a load cell and as a harmonic current is applied to the electromagnet, a magnetic force is formed between the permanent magnet and the electromagnet that is proportional to the magnetic field generated by the coil, this setup is shown in Fig. 11. While not ideal, this test can effectively identify the relation between the applied current and the magnetic field generated.

The results of the experiment performed showed the dynamic response of the electromagnetic coil to clearly cause a variation in the response with respect to frequency. The frequency response of the experimental setup was measured as the coil was magnetized using a swept sine wave, a typical frequency response is shown in

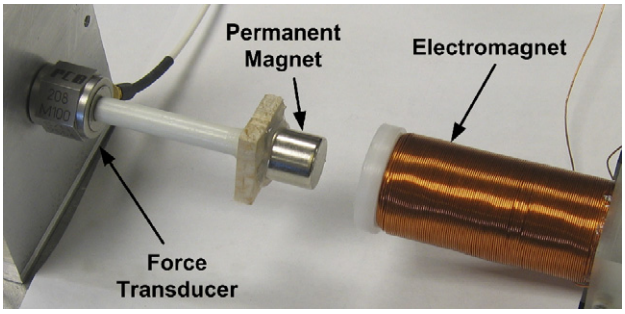

Fig. 11. Experimental setup used to measure the magnetic field generated by the permanent magnet.

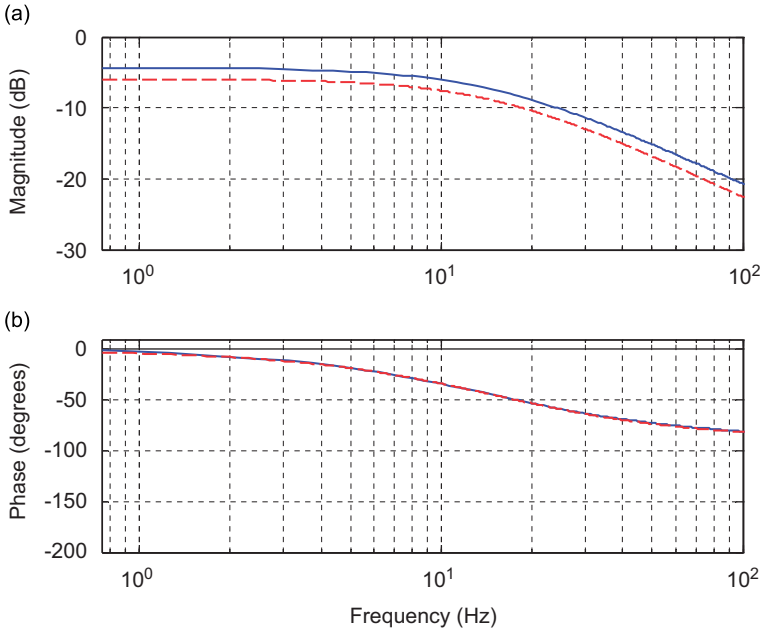

Fig. 12. Frequency response of coil and frequency response of a transfer function with a single pole at 15 Hz indicating their match: (a) magnitude, (b) phase. --, simulated frequency response; and -, experimental frequency response of coil.

Fig. 12. The frequency response shows that the electromagnetic coil has a break frequency at 15 Hz, after which the magnetic force generated has 20 dB attenuation per decade as the frequency is increased. These two characteristics of the frequency response can be modeled as a transfer function with a cut-off frequency at 15 Hz and are plotted in Fig. 12. The small offset in the magnitude is intentionally placed to show the two curves are identical, and should not match because the experimental system does not represent the forces generated in the eddy current control system. The purpose of the experiment is simply to identify the pole location of the electromagnetic coil. Using this quantity, the frequency response of the coil can be included in the model to increase its accuracy.

The frequency responses predicted by the theoretical model when the dynamics of the electromagnetic coil are included in the simulation, compared to the measured frequency response, are shown in Fig. 13. The figure shows that with the dynamics of the electromagnet included, the model provides a better estimate of the frequency response and the second mode no longer has a shift in the magnitude of the controlled response. The filter parameters used to apply control to each mode for the theoretical model that includes the magnet dynamics, and experiments are provided in Table 2. From this table, it can be seen that all tuned parameters used in the theory are almost identical to those used in the experiments. These results indicate that the source of error in the previously calculated frequency response was due to the phase shift between the current applied to the coil and the resulting magnetic field. From Fig. 13, it can be seen that the active control scheme is very effective for use as a vibration suppression tool. This system has reduced the cantilevers beam's first mode of vibration by more than 97.5% and the second mode of vibration by 96.5%. This illustrates the significant vibration control that can be delivered to the system. Furthermore, this method allows vibration control forces to be applied to the structure without contacting the structure, thus avoiding mass loading and added stiffness

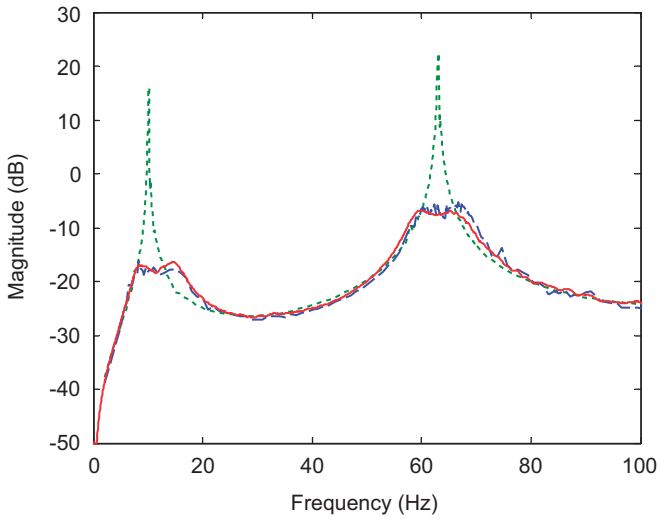

Fig. 13. Controlled response of the beam's first two bending modes compared to the uncontrolled case when the transfer function of the electromagnet is included. ••, Uncontrolled, --, experimental controlled response, and -, predicted controlled response.

Table 2
Filter parameter used in the experiments and predicted by the theoretical simulation when the transfer function of the coil is included

	First mode		Second mode	
	Measured	Predicted	Measured	Predicted
Filter frequency	$1.37\omega_1$	$1.37\omega_1$	$0.987\omega_2$	$0.98\omega_2$
Filter damping	0.34	0.4	0.1	0.1
Filter gain	−4	−5	−0.005	−0.005

which are downfalls of other actuation methods. The non-contact properties of this actuation method are desirable in many different types of structures; however, they are particularly well suited for use with the extremely flexible systems intended for use in future space applications, including solar sails and deployable satellites. These structures are difficult to control because their high flexibility limits point actuation methods and the use of membranes as metrology surfaces causes bonding of actuators to result in surface aberrations. Additionally, the control forces can be greater than those of electrostatic methods.

Once the response of the controlled system has been tuned in the frequency domain, the effectiveness of the active control system and accuracy of the model can be identified in the time domain. To demonstrate the performance of the control system, the beam is excited at its natural frequency without control; the controller is then instantaneously turned on allowing the beam to be suppressed into its closed loop response. By looking at the time response of the system when vibrating in its uncontrolled steady state and when the controller is tuned on, both the settling time and the overall attenuation of the beam can easily be seen. The predicted and measured time response of the first mode when the controller is turned on at 2.0 s is provided in Fig. 14, and the typical time response of the second mode when the controller is turned on at 1.5 s is shown in Fig. 15. These figures show that the predicted time response shows the same settling time and vibration suppression (93.3% measured and 94.6% predicted suppression) as the measured response and demonstrates that the active eddy current control system can suppress the beam's first mode of vibration by 94.6% and the second mode of vibration by 96.6%.

A passive–active control system was developed by Sodano et al. [10] that used an actuator to actively control the velocity of a permanent magnet relative to the motion of the vibrating structure. Therefore, eddy currents were formed in the conductor due to the net velocity between the conductor and the permanent magnet. This system functioned in a completely non-contact way and was shown to possess a large control authority over the structure; however, the damper required an actuation system to displace the magnet relative the vibrating structure. The requirement for this additional actuation system limited the bandwidth of the controller to that of the actuator. The study performed in Ref. [10] used an electromagnetic shaker to displace the magnet, whose magnitude of displacement rolls of at higher frequencies, this choice of actuation method only allowed the first two modes of vibration to be controlled. The active eddy current damping system that has been described in this manuscript also functions in a non-contact manor and does not require any additional actuation devices allowing it to easily apply control to higher frequency modes. The ability of the

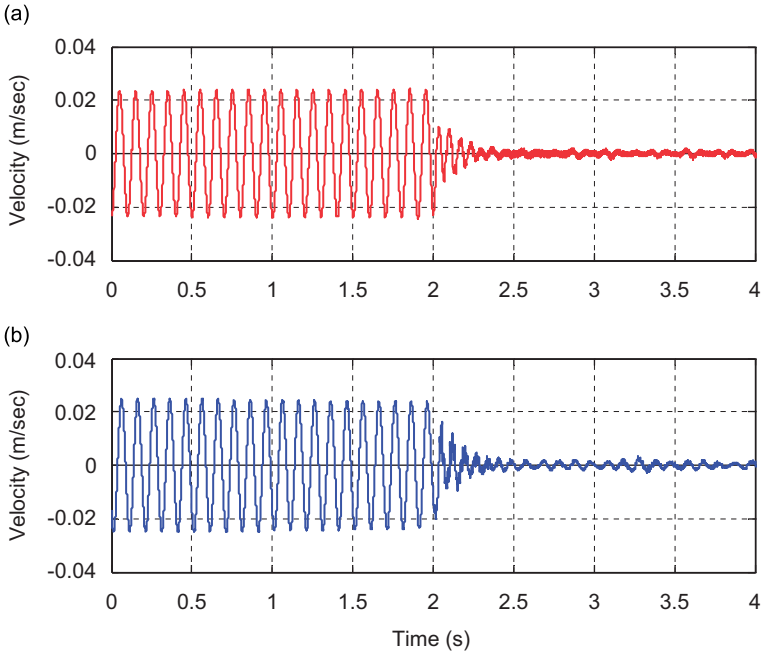

Fig. 14. Time response of the beam excited at its first bending mode with the controller turned on at 2.0 s: (a) predicted and (b) measured.

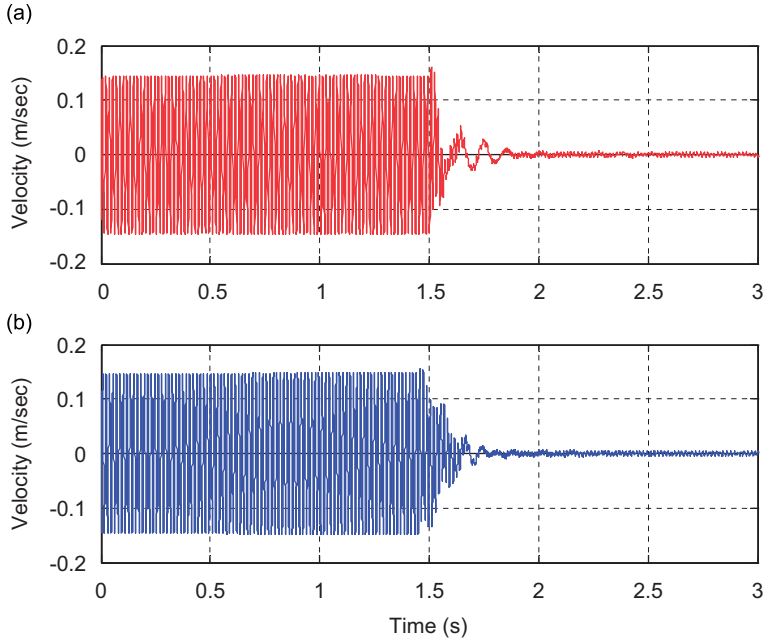

Fig. 15. Time response of the beam excited at its second bending mode with the controller turned on at 1.5 s: (a) predicted and (b) measured.

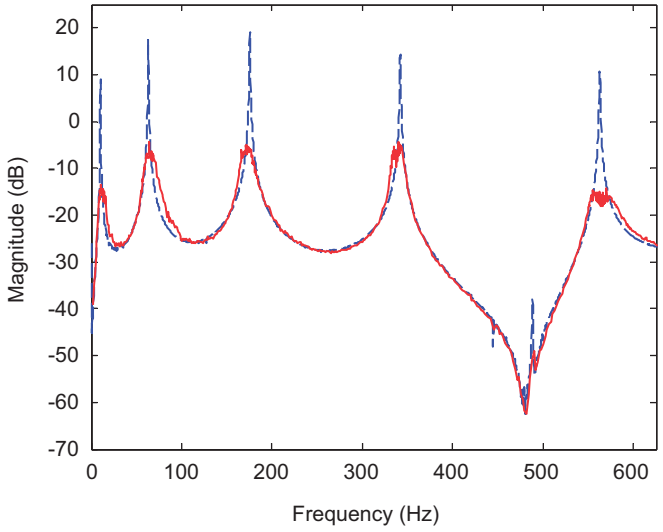

Fig. 16. Experimental control of the beam's first five modes: - -, uncontrolled and -, controlled.

active system to suppress higher frequency modes can be seen in Fig. 16, which shows the frequency response of the beam when no control is applied and when the first five modes of vibration and controlled. From the figure it can be seen that each of the first five modes of vibration is suppressed by approximately 20 dB, thus illustrating that the active eddy current control system can effectively apply control to higher frequency modes.

Once the improved bandwidth of the active eddy current controller had been demonstrated, the active system's ability to suppress an initial disturbance was compared to that of the passive–active system described in Ref. [10]. The test was performed by displacing the beam a constant amount using an electromagnet to attract the beam, then the electromagnet was de-energized and the beam was released from its initial

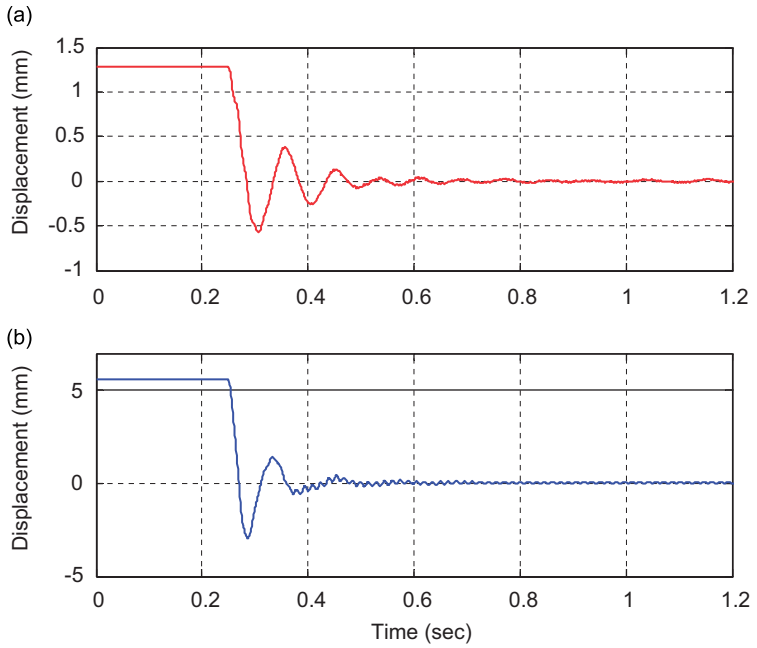

Fig. 17. Controlled initial displacement response of the cantilever beam: (a) with the active controller and (b) with the passive–active damper developed by Sodano et al. [10].

displacement and allowed to vibrate freely. Once the beam begins to vibrate, the controller works to quickly suppress the vibration. A typical experimentally measured controlled response to an initial condition is shown in Fig. 17 for both the passive–active system, and the fully active system. From this figure, it can be seen that the active control system can effectively suppress the vibration of the beam, and that the settling time is comparable to that of the passive–active damper of Ref. [10]. Therefore, in addition to having a larger bandwidth than the passive–active controller, the active system is much smaller and can effectively suppress an initial disturbance.

5. Conclusions

The eddy currents formed when a conductive material is subjected to a time varying magnetic field can be used to generate controlled forces for the suppression of vibration. By sensing the velocity of the vibrating structure and actively modifying the current flowing through the coil a time-changing magnetic field is generated that induces eddy currents in the conductor and results in a magnetic force. This actuation method is novel because it is completely non-contact. Therefore, control forces can applied be to the structure without inducing the mass loading or added stiffness that are common downfalls of other actuation techniques. The non-contact nature of this actuation technique is desirable in many different applications, however it is particularly well suited for use with the extremely flexible metrology surfaces to be used in future space missions, including solar sails and deployable satellites. These structures are difficult to control due to the stringent surface tolerances that can easily be compromised by the surface aberrations that result from bonding of actuators to the metrology surface or the use of a point actuation method. The actuator used in this study had significant mass; however, it could be miniaturized for applications requiring low forces, such as thin membranes. Furthermore, the control system can be easily incorporated into the system and the forces can be greater than those generated by electrostatic actuators.

The effective use of an active eddy current actuator for the suppression of transverse vibrations has been demonstrated in this work. Non-contact actuators of this kind have not been previously investigated and this is the first study to present its use. Additionally, the necessary design considerations for the controller have been presented. It was shown that the theoretical model of the active control system using a single

electromagnet placed a small distance from a conductive structure as the actuation source provides an accurate prediction of the closed-loop response. This actuation method generates a magnetic force between the conductor and electromagnet at twice the frequency of the current applied to the coil. This effect results in the need for a control algorithm to reduce the frequency of the sensing signal by half such that the force applied to the structure is capable of suppressing the system's vibration. The controller was designed to compensate for this nonlinearity, allowing it to effectively function as a non-contact vibration sensor. Experiments were then performed on a cantilever aluminum beam to demonstrate the control systems effectiveness. The results of the experiments showed the theoretical model of the electromagnetic vibration control system to very accurately predict the system's dynamic response. The control system was shown to suppress each of the beams first five modes of vibration by upwards of 20 dB. These results showed that the control system provides increased bandwidth over previously used eddy current vibration control systems and dampers. Additionally, the performance of the controller was demonstrated in the time domain illustrating high control authority and the system's effectiveness in suppressing an initial displacement.

Appendix A. Integrals defining the magnetic flux

The integration I_1 in Eq. (7) is

$$I_1 = \int_0^{2\pi} \frac{\sin\,\phi}{(b^2+z^2-2yb\,\sin\,\phi)^{2/3}}\,\mathrm{d}\phi = \frac{1}{bynp^2}\left[m^2\left\{E_1\left(\frac{\pi}{4},\frac{-4yb}{n^2}\right)+E_1\left(\frac{3\pi}{4},\frac{-4yb}{n^2}\right)\right\}-p^2\left\{E_2\left(\frac{\pi}{4},\frac{-4yb}{n^2}\right)+E_2\left(\frac{3\pi}{4},\frac{-4yb}{n^2}\right)\right\}\right], \quad \text{(A.1)}$$

where

$$m^2 = b^2+y^2+z^2, \quad \text{(A.2)}$$

$$n^2 = (b-y)^2+z^2, \quad \text{(A.3)}$$

$$p = (b+y)^2+z^2. \quad \text{(A.4)}$$

The elliptic integrals of Eq. (A.1) are

$$E_1 = (\phi,m) = \int_0^{\phi}(1-m\sin^2\theta)^{1/2}\,\mathrm{d}\theta, \quad \text{(A.5)}$$

$$E_2 = (\phi,m) = \int_0^{\phi}(1-m\sin^2\theta)^{-1/2}\,\mathrm{d}\theta. \quad \text{(A.6)}$$

The integration I_2 in Eq. (8) is

$$I_2 = \int_0^{2\pi} \frac{b-y\,\sin\,\phi}{(b^2+z^2-2yb\,\sin\,\phi)^{2/3}}\,\mathrm{d}\phi = \frac{1}{bnp^2}\left[s\left\{E_1\left(\frac{\pi}{4},\frac{-4yb}{n^2}\right)+E_1\left(\frac{3\pi}{4},\frac{-4yb}{n^2}\right)\right\}+p^2\left\{E_2\left(\frac{\pi}{4},\frac{-4yb}{n^2}\right)+E_2\left(\frac{3\pi}{4},\frac{-4yb}{n^2}\right)\right\}\right], \quad \text{(A.7)}$$

where

$$m^2 = b^2+y^2+z^2, \quad \text{(A.8)}$$

$$n^2 = (b-y)^2+z^2, \quad \text{(A.9)}$$

$$p = (b+y)^2+z^2, \quad \text{(A.10)}$$

$$s = b^2-y^2-z^2. \quad \text{(A.11)}$$

The elliptic integrals of Eq. (A.7) are

$$E_1 = (\phi, m) = \int_0^{\phi} (1 - m \sin^2 \theta)^{1/2} \, \mathrm{d}\theta, \tag{A.12}$$

$$E_2 = (\phi, m) = \int_0^{\phi} (1 - m \sin^2 \theta)^{-1/2} \, \mathrm{d}\theta. \tag{A.13}$$

References

[1] D. Karnopp, Permanent magnet linear motors used as variable mechanical damper for vehicle suspensions, *Vehicle System Dynamics* 18 (1989) 187–200.

[2] M. Schmid, P. Varga, Analysis of vibration-isolating systems for scanning tunneling microscopes, *Ultramicroscopy* 42–44 (1992) 1610–1615.

[3] H. Teshima, M. Tanaka, K. Miyamoto, K. Nohguchi, K. Hinata, Effect of Eddy current dampers on the vibrational properties in superconducting levitation using melt-processed YbaCuO bulk superconductors, *Physica C* 274 (1997) 17–23.

[4] M.K. Kwak, M.I. Lee, S. Heo, Vibration suppression using eddy current damper, *Korean Society for Noise and Vibration Engineering* 13 (10) (2003) 760–766.

[5] J.S. Bae, M.K. Kwak, D.J. Inman, Vibration suppression of cantilever beam using eddy current damper, *Journal of Sound and Vibration* 284 (3–5) (2005) 805–824.

[6] H.A. Sodano, J.S. Bae, Eddy current damping in structures, *Shock and Vibration Digest* 36 (6) (2004) 469–478.

[7] H.A. Sodano, J.S. Bae, D.J. Inman, W.K. Belvin, Concept and model of eddy current damper for vibration suppression of a beam, *Journal of Sound and Vibration* 288 (4–5) (2005) 1177–1196.

[8] H.A. Sodano, J.S. Bae, D.J. Inman, W.K. Belvin, Modeling and application of passive eddy current damper for the suppression of membrane vibrations, *AIAA Journal* 44 (3) (2006) 541–549.

[9] H.A. Sodano, J.S. Bae, D.J. Inman, W.K. Belvin, Improved concept and model of eddy current damper, *Journal of Vibration and Acoustics—Transactions of the ASME* 128 (2006) 295–302.

[10] H.A. Sodano, D.J. Inman, W.K. Belvin, Development of a new passive-active magnetic damper for vibration suppression, *Journal of Vibration and Acoustics—Transactions of the ASME* 128 (2006) 318–327.

[11] J. Tani, M. Minagawa, K. Ohtomo, M. Saigo, Dynamic behavior of thin plates under impulsive magnetic field, *IEEE Transactions on Magnetics* 26 (2) (1990) 544–547.

[12] T. Morisue, Analysis of a coupled problem: the felix cantilevered beam, *IEEE Transactions on Magnetics* 26 (2) (1990) 540–543.

[13] H. Tsubi, M. Tanaka, T. Misaki, Eddy current and deflection analysis of a thin plate in time-changing magnetic fields, *IEEE Transactions on Magnetics* 26 (5) (1990) 1647–1649.

[14] T. Takagi, J. Tani, S. Matsuda, S. Kawamura, Analysis and experiment of dynamic deflection of a thin plate with a coupling effect, *IEEE Transactions on Magnetics* 28 (2) (1992) 1259–1262.

[15] T. Takagi, J. Tani, Dynamic behavior of a plate in magnetic field by full coupling and MMD methods, *IEEE Transactions on Magnetics* 30 (5) (1994) 3296–3299.

[16] J.S. Lee, Dynamic stability of beam plates in transverse magnetic fields, *Journal of Engineering Mechanics* 122 (2) (1996) 89–94.

[17] H.A. Sodano, D.J. Inman, Modeling of a new active eddy current vibration control system, *Journal of Dynamic Systems, Measurement and Control—Transactions of the ASME* (2006), in press.

[18] J.L. Fanson, T.K. Caughey, Positive position feedback control for large space structures, *AIAA Paper No. 87-0902, Proceeding of the 28th AIAA/ASME/ASCE/AHS Structures, Structural Dynamics and Materials Conference*, Monterey, CA, April 9–10, 1987, pp. 588–598.